Cell Death and Differentiation (2016) 23, 430–441

www.nature.com/cdd

An essential role for Ink4 and Cip/Kip cell-cycle inhibitors in preventing replicative stress

V Quereda[1], E Porlan[1], M Cañamero[2], P Dubus[3] and M Malumbres*[,1]

Cell-cycle inhibitors of the Ink4 and Cip/Kip families are involved in cellular senescence and tumor suppression. These inhibitors are individually dispensable for the cell cycle and inactivation of specific family members results in increased proliferation and enhanced susceptibility to tumor development. We have now analyzed the consequences of eliminating a substantial part of the cell-cycle inhibitory activity in the cell by generating a mouse model, which combines the absence of both $p21^{Cip1}$ and $p27^{Kip1}$ proteins with the endogenous expression of a Cdk4 R24C mutant insensitive to Ink4 inhibitors. Pairwise combination of Cdk4 R24C, p21-*null* and p27-*null* alleles results in frequent hyperplasias and tumors, mainly in cells of endocrine origin such as pituitary cells and in mesenchymal tissues. Interestingly, complete abrogation of $p21^{Cip1}$ and $p27^{Kip1}$ in Cdk4 R24C mutant mice results in a different phenotype characterized by perinatal death accompanied by general hypoplasia in most tissues. This phenotype correlates with increased replicative stress in developing tissues such as the nervous system and subsequent apoptotic cell death. Partial inhibition of Cdk4/6 rescues replicative stress signaling as well as p53 induction in the absence of cell-cycle inhibitors. We conclude that one of the major physiological activities of cell-cycle inhibitors is to prevent replicative stress during development.

Cell Death and Differentiation (2016) **23,** 430–441; doi:10.1038/cdd.2015.112; published online 21 August 2015

The involvement of cell-cycle regulators in human cancer has been extensively studied in the last years.[1–3] The retinoblastoma protein (pRb) pathway has a key role in the regulation of these cellular processes, and this protein as well as its regulators—cyclins, cyclin-dependent kinases (Cdks) and Cdk inhibitors—are frequently deregulated in human cancer.[2] In quiescent cells, pRb represses the transcription of genes required for DNA replication or mitosis. This function is achieved through the sequestering of inactive E2F transcription factors and through the binding to histone deacetylases and chromatin remodeling complexes. Upon mitogenic stimuli, D-type cyclins are induced and activate the cell-cycle kinases Cdk4 and Cdk6. Cyclin D-Cdk4/6 complexes phosphorylate and partially inactivate pRb, allowing the expression of E2F-target genes.[4]

Whereas mitogenic stimuli induce cyclins and therefore activate Cdks, antimitogenic signals prevent cell-cycle progression by inducing members of two families of Cdk inhibitors (CKIs), the Ink4 and Cip/Kip families.[5] Members of the Ink4 family, $p16^{Ink4a}$, $p15^{Ink4b}$, $p18^{Ink4c}$ and $p19^{Ink4d}$, specifically bind Cdk4 and Cdk6 inhibiting their catalytic activity by allosteric competition of their binding with cyclins. On the other hand, Cip/Kip family members, $p21^{Cip1}$, $p27^{Kip1}$ and $p57^{Kip2}$, are able to bind and inhibit several Cdk–Cyclin complexes.[5] Ink4 and Cip/Kip proteins display tumor suppressor activity and are frequently inactivated in human tumors by different mechanisms.[2,6] Individual genetic ablation of $p16^{Ink4a}$, $p15^{Ink4b}$, $p18^{Ink4c}$, $p21^{Cip1}$ or $p27^{Kip1}$ leads to increased susceptibility to lymphomas, sarcomas, and some other tumor types such as endocrine neoplasias.[7–15] Elimination of individual inhibitors has a limited effect probably due to possible compensation by the remaining family members.[11,16] Stronger cooperation is usually found when Ink4 and Cip/Kip alterations are combined. For instance, combination of $p16^{Ink4a}$ or $p18^{Ink4c}$ ablation with $p27^{Kip1}$ deficiency synergizes in lymphoma or pituitary tumor development.[15,17] A more detailed analysis of the effects of a general inactivation of Cdk inhibitors has not been possible so far due to the limitations of combining a high number of genetic alterations in the mouse.

Whereas Cip/Kip proteins have been suggested to display multiple activities in addition to Cdk inhibition, Ink4 proteins are thought to function mostly, if not uniquely, by inhibiting the activity of Cdk4 and Cdk6.[4,5] A mutation in the Cdk4 kinase that prevents the effect of Ink4 inhibitors, change of arginine R24 to cysteine (R24C), was found to contribute to melanoma development.[18] *Knock-in* mice harboring the Cdk4 R24C allele develop a wide spectrum of tumors due to the lack of inhibitory effect of Ink4 proteins on this kinase.[19,20] The Cdk4 R24C mutation cooperates with the lack of $p27^{Kip1}$ (ref. 21) or the lack of $p21^{Cip1}$ (ref. 22) in the susceptibility to tumor development, but not with the lack of $p18^{Ink4c}$,[21] in agreement with the idea that the R24C mutation results in resistance to Ink4 function. Yet, the cooperation between the Cdk4 R24C allele and lack of either $p21^{Cip1}$ or $p27^{Kip1}$ only affects to specific tumor types (sarcoma or pituitary neoplasia, respectively) and most other tissues are unaffected.

[1]Cell Division and Cancer Group, Molecular Oncology Programme, Spanish National Cancer Research Centre (CNIO), Madrid, Spain; [2]Histopathology Unit, Biotechnology Programme, CNIO, Madrid, Spain and [3]EA2406 Histology and Molecular Pathology of Tumours, University of Bordeaux 2, Bordeaux, France
*Corresponding author: M Malumbres, Cell Division and Cancer Group, Centro Nacional de Investigaciones Oncológicas (CNIO), Melchor Fernández Almagro 3, Madrid 28029, Spain. Tel: +34 91 224 6900; Fax: +34 91 732 8033; E-mail: malumbres@cnio.es
Abbreviations: AC3, active caspase 3; Cdk, cyclin-dependent kinase; CKI, Cdk inhibitor; E, embryonic day; P, postnatal day; R, R24C mutation in Cdk4; Rb, retinoblastoma; pRb, retinoblastoma protein
Received 22.1.2015; revised 15.6.2015; accepted 09.7.2015; Edited by A Villunger; published online 21.8.15

To understand the possible compensatory effects between Cip/Kip and Ink4 proteins, we have now combined both the p21- and p27-null alleles with a Cdk4 R24C background. Mice with intermediate genotypes display a gradual increase in tumor susceptibility when several mutant alleles are combined. Surprisingly, genetic combination of these three alterations results in perinatal lethality accompanied of general hypoplasia with severe proliferative defects in multiple tissues. This phenotype is not due to the presence of early tumors but to a general, p53-dependent, hypoproliferative defect caused by replicative stress generated in the absence of these inhibitors. These data suggest that cell-cycle inhibitors are primarily needed to moderate the activity of Cdks and prevent replicative stress during the formation of tissues in late development.

Results

Genetic cooperation between Cdk4 R24C and lack of Cip/Kip inhibitors. We analyzed the effect of the combined ablation of $p21^{Cip1}$ and $p27^{Kip1}$ in a Cdk4 R24C background using a triple mutant mouse model. As reported previously, lack of $p27^{Kip1}$ strongly cooperated with the Cdk4 R24C [*Cdk4*(R)] allele whereas the absence of $p21^{Cip1}$ resulted in a

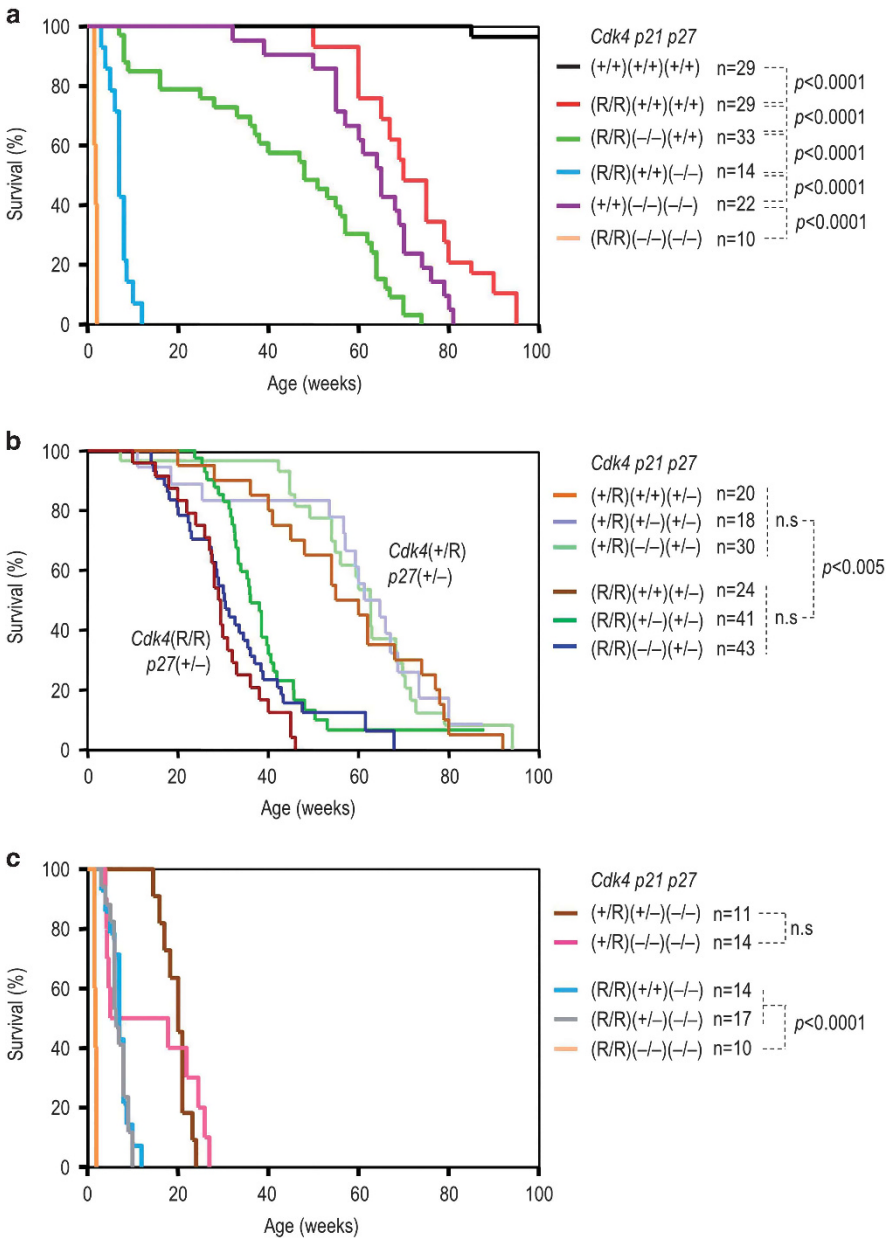

Figure 1 Survival of mice with combined Cdk4 R24C; p21-null and p27-null alleles. (**a**) Survival of mice homozygous for the different alleles: Cdk4 R24C [*Cdk4*(R)], $p21^{Cip1}$-null [*p21*(–)], and $p27^{Kip1}$-null [*p27*(–)], double homozygous or triple mutants. (**b**) Comparative representation of the effect of $p21^{Cip1}$ ablation in heterozygous or homozygous Cdk4 R24C mutants in a $p27^{Kip1}$ heterozygous background. (**c**) Comparison of the survival of the most aggressive genotypes characterized by a *p27*(–/–) background. Statistically significant differences between different groups are shown. n.s., not significant ($P > 0.01$; log-rank (Mantel-Cox) test)

moderate but significant decrease in survival in a Cdk4 R24C background (Figure 1a; Sotillo *et al*.[19,21] and Quereda *et al*.[22]). The combined ablation of $p21^{Cip1}$ and $p27^{Kip1}$ led to perinatal lethality in *Cdk4*(R/R) mice (median lifespan = 2 weeks; Figure 1a) whereas $p21^{Cip1}$;$p27^{Kip1}$ double *knock-out* mice were viable and developed similar pathologies to single mutants in a *Cdk4*-wild-type background (Table 1; Garcia-Fernandez *et al*.[23]). Gradual ablation of $p21^{Cip1}$ displayed no significant impact in *Cdk4*(+/R) or *Cdk4*(R/R) mice carrying a single copy of $p27^{Kip1}$ (Figure 1b). Complete absence of $p27^{Kip1}$ had a major effect in *Cdk4*(+/R) or *Cdk4*(R/R) mice, which died within the first 7 months of life. In that background, lack of the two alleles of $p21^{Cip1}$ resulted in earlier lethality (although not statistically significant) and *Cdk4*(+/R); *p21*(–/–); *p27*(–/–) mice displayed a median lifespan of 6 weeks (50% of the colony died before this age) *versus* 21 weeks in *Cdk4*(+/R); *p21*(+/–); *p27*(–/–) mice. Similarly, *Cdk4*(R/R); *p21*(+/–); *p27*(–/–) mice displayed a median lifespan of 8 weeks while complete lack of $p21^{Cip1}$ significantly reduced this value to 2 weeks in *Cdk4*(R/R); *p21* (–/–); *p27*(–/–) mice (Figure 1c; Table 1).

Histopathological studies of these compound mice revealed diverse pathologies which incidence and latency varied with the genotype (Table 1). Angiosarcomas and pituitary tumors were the most prevalent pathologies although single or double mutants also developed other epithelial or mesenchymal tumors. As lifespan of these models decrease, pituitary tumors stood as the most prevalent pathology and was the only tumor observed in genotypes whose lifespan is lower than 20 weeks of life [*Cdk4*(+/R); *p21*(–/–); *p27*(+/–); *Cdk4*(+/R); *p21*(–/–); *p27*(–/–); *Cdk4*(R/R); *p21*(+/+); *p27*(–/–) and *Cdk4*(R/R); *p21* (+/–); *p27*(–/–)]. Although the development of pituitary tumors was led by the *Cdk4*(R) and *p27*(–) alleles, lack of $p21^{Cip1}$ also cooperated in this pathology in the presence of wild-type alleles of either *Cdk4* or *$p27^{Kip1}$*. These pituitary tumors were usually accompanied with hyperplasia of other endocrine tissues, such as the Langerhans islets in the pancreas or adrenal gland, as well as hyperplasia of Leydig cells in the testis (Supplementary Table S1 and Supplementary Figure S1). The aberrations in the pituitary gland, frequently altered in mouse models of cell-cycle deregulation,[24] are summarized in Table 1 and Supplementary Table S2. Lack of $p27^{Kip1}$, or the combined loss of $p21^{Cip1}$ and $p27^{Kip1}$, resulted in pars intermedia tumors whereas the activating R24C mutation in Cdk4 generated tumors in the pars distalis (Supplementary Table S2; Sotillo *et al*.[19]). Combination of the *$Cdk4^{R24C}$*;*p21*(–) and *p27*(–) alleles resulted in a variety of pituitary pathologies affecting both localizations. Moreover, the more aggressive combination of mutant alleles [*Cdk4*(R/R); *p21*(+/+); *p27*(–/–) and *Cdk4*(R/R); *p21*(+/–); *p27*(–/–)] resulted in about 70% of undifferentiated pituitary neoplasias whose cell-of-origin was difficult to assess. These tumors were characterized by the presence of giant neuron-like cells negative for neuronal markers such as NeuN (data not shown), as well as small endocrine-like cells (Supplementary Figure S1). These tumors also presented regions positive for hormone markers such as growth hormone, follicular stimulating hormone or prolactin but where mostly negative for thyroid-stimulating hormone (Supplementary Figure S1 and data not shown).

Table 1 Percentage of spontaneous tumors in Cdk4 R24C; $p21^{Cip1}$; $p27^{Kip1}$ mutant mice

Tumor type	*Cdk4*(+/+) *p21*(+/+) *p27*(+/+)	(+/+) (–/–) (–/–)	(+/R) (+/–) (+/–)	(+/R) (–/–) (+/–)	(+/R) (+/–) (–/–)	(+/R) (–/–) (–/–)	(R/R) (+/+) (+/+)	(R/R) (–/–) (+/+)	(R/R) (+/–) (+/–)	(R/R) (–/–) (+/–)	(R/R) (+/+) (–/–)	(R/R) (+/–) (–/–)	(R/R) (–/–) (–/–)
	N = 23	*N* = 22	*N* = 6	*N* = 17	*N* = 6	*N* = 10	*N* = 21	*N* = 19	*N* = 25	*N* = 20	*N* = 7	*N* = 10	*N* = 6
Angiosarcoma	0	9	50	35	0	0	56	47	20	25	0	0	0
Osteosarcoma	0	0	0	0	0	0	1	11	0	0	0	0	0
Squamous cell carcinoma	0	0	0	0	0	0	0	5	0	5	0	0	0
Lung, pneumocyte type II adenoma	0	0	0	0	0	0	18	11	0	0	0	0	0
Pancreatic endocrine	0	0	0	0	0	0	31	21	20	0	0	0	0
Pituitary	0	46	83	53	83	50	22	21	96	60	100	90	0
Lymphoma	5	5	0	0	0	0	2	7	4	0	0	0	0
Pheochromocytoma	0	14	0	0	0	0	0	0	0	0	0	0	0
Leydig cell[a]	0	0	0	38	0	0	0	0	46	15	0	0	0
Tumor free (%)[b]	80	73	0	0	17	50	6	0	0	20	0	10	100
Median survival (weeks)	> 100	52	58.5	52	19.6	22	72.5	53.7	36.4	28.9	7	6.1	2

[a]Percentage of Leydig cell tumors in males. [b]Percentage of mice without tumors at death (this number does not simply derives from the sum of the pathologies above since a mouse may have several tumors).

Inactivation of Ink4, p21^{Cip1} and p27^{Kip1} inhibitors results in perinatal lethality in the absence of tumors. Interestingly, despite the high incidence of tumors in mice with these aggressive genotypes, the complete absence of both p21^{Cip1} and p27^{Kip1} inhibitors in a Cdk4^{R24C} background resulted in early lethality in the absence of tumors or obvious hyperplasia (Figure 1; Table 1). *Cdk4*(R/R); *p21*(–/–); *p27*(–/–) mice were born at the expected mendelian ratio and had normal appearance as compared with their control littermates at the moment of the birth. However, by 2 weeks of age, they presented a significantly reduced weight compared with their littermates (4.1 ± 0.8 g *versus* 8.7 ± 0.5 g) and reduced motility (Figure 2a; Supplementary Video S1). These phenotypes became more evident in the following few days and *Cdk4*(R/R); *p21*(–/–); *p27*(–/–) mice died before the third week of age (Figure 1). Histopathological analysis of these animals revealed several developmental defects represented by massive hypoplasia in tissues such as bone marrow or lung (Figure 2b). The pituitary gland of triple mutant mice was smaller than that of control littermates, without obvious differences in the percentage of hormone-producing cells or progenitor cells as determined by Sox2 (not shown) or Sox9 staining (Figure 2c). Triple mutant *Cdk4*(R/R); *p21*(–/–); *p27*(–/–) pituitaries displayed no significant differences in the ratio of Ki67-positive cells at this stage but showed a significant increase in the number of apoptotic cells, as detected by antibodies against the active form of caspase 3 (Figure 2d). Although the degree of proliferation (as measured by Ki67 staining) varies among the different tissues and genotypes, there is a consistent increase in apoptosis in triple mutant mice (Figure 3). These data suggest that, although the partial combination of these mutant alleles displays a variable effect on proliferation depending on the tissue, complete ablation of p21^{Cip1} and p27^{Kip1} in the Cdk4 R24C background results in a unique apoptotic phenotype.

Ink4 and Cip/Kip inhibitors cooperate preventing replicative stress. We then focused to the developing nervous system, a tissue that displays high levels of proliferation in utero that gradually decease after birth. Histological examination of E17.5 brains showed an increase in the percentage of the mitotic marker phospho-histone H3 (Supplementary Figure S2). At death, P15 *Cdk4*(R/R); *p21*(–/–); *p27*(–/–) mice presented an slight but significant increase in the proliferation of the subgranular zone of the dentate gyrus on the hippocampus (Figure 4) and in the subependymal zone (Figure 5), two regions that maintain neural progenitors after birth. Hyperproliferation was accompanied by induction of apoptotic cell death as measured by active caspase 3. This signal also coexisted with immunostaining for p53 proteins phosphorylated in Ser15, a marker already observed in E17.5 brains (Supplementary Figure S2). This residue is phosphorylated by checkpoint kinases ATM and ATR, suggesting the activation of a DNA damage-like response. Since these animals were not exposed to exogenous damage, we then checked for replication defects as a possible cause of cell death. Pan-nuclear intense staining of phosphorylated H2AX (γH2AX) or increased phosphorylation of RPA was observed in triple mutant brains but not in control animals at both ages examined (Figures 4 and 5; Supplementary Figure S2). This type of staining is characteristic of replicative stress rather than genotoxic damage characterized by the presence of multiple but individual γH2AX foci in the nucleus. This replicative stress and the subsequent apoptotic cell death was not obvious at mid gestation (E14.5, data not shown) but gradually increased from E17.5 until P15 (Figure 5). Furthermore, we noticed an increase in GFAP-positive cells in the brain (Supplementary Figure S3), a sign of reactive gliosis commonly found after brain injury. Reactive gliosis was particularly abundant in the habenula, an area involved in learning and stress responses among other functions, in line with the defects in behavior and motility (Supplementary Videoes S1 and S2). All together these data suggest that the deregulation of the cell cycle starts at late developmental embryonic stages and has cumulative effects resulting in major defects in brain development accompanied by perinatal death in triple mutant mice.

Defective self-renewal of mutant neural progenitors *in vitro*. We then analyzed the relevance of these cell cycle inhibitors in self-renewal and proliferation of neural progenitors in culture. Embryonic (E18.5) neural progenitors were isolated from crosses between animals with compound genotypes, and cultured in neurosphere-forming conditions for over a week. A normalized analysis revealed that primary neurosphere formation was drastically reduced by the Cdk4 R24C allele when compared with Cdk4-wild-type littermate neural progenitors (Figures 6a–c). Lack of both p21^{Cip1} and p27^{Kip1} in a wild-type background resulted in a significant increase in primary neurosphere formation that was not present in the single knock-out cells. The concomitant inactivation of Ink4 inhibitors in the *Cdk4*(R/R) background prevented the effect of p21/p27 ablation in the number of neurospheres and, to a lesser extent, in their size (Figures 6a–c). The defects in primary neurosphere formation in the presence of the Cdk4 R24C alleles actually occurred with independence of the levels of Cip/Kip inhibitors. When primary neural progenitors were disaggregated under papain and reseeded in self-renewal conditions, very few secondary spheres were found in the triple mutant genotype, while all the other genotypes consistently formed neurospheres at variable frequencies (Figures 6d and e). This suggests a cooperative effect between the lack of Ink4 and Cip/Kip inhibitors that is only obvious after a few cell divisions in the neural progenitors.

Primary neurospheres were then incubated with the nucleotide analog EdU and immunofluorescence was performed for different markers (Figure 6f). Most dividing cells (EdU positive) were positive for Sox9 marker, whereas Sox9-negative cells were negative for EdU suggesting the presence in the neurospheres of a population of differentiated cells with reduced proliferative potential. *Cdk4*(R/R); *p21*(+/+); *p27*(+/+) displayed defective growth (Figure 6c) and decreased EdU incorporation (Figure 6f), likely as a consequence of the increase in p21^{Cip1} and p27^{Kip1} inhibitors in these mutant cells (Supplementary Figure S4). However, we observed a significant increase in the percentage of Sox9-positive cells in the triple mutant compared with wild-type neural progenitors. This observation correlated with published data suggesting that a diminished G1 phase may result in an increase of basal progenitors generation in brain.[25] Although not

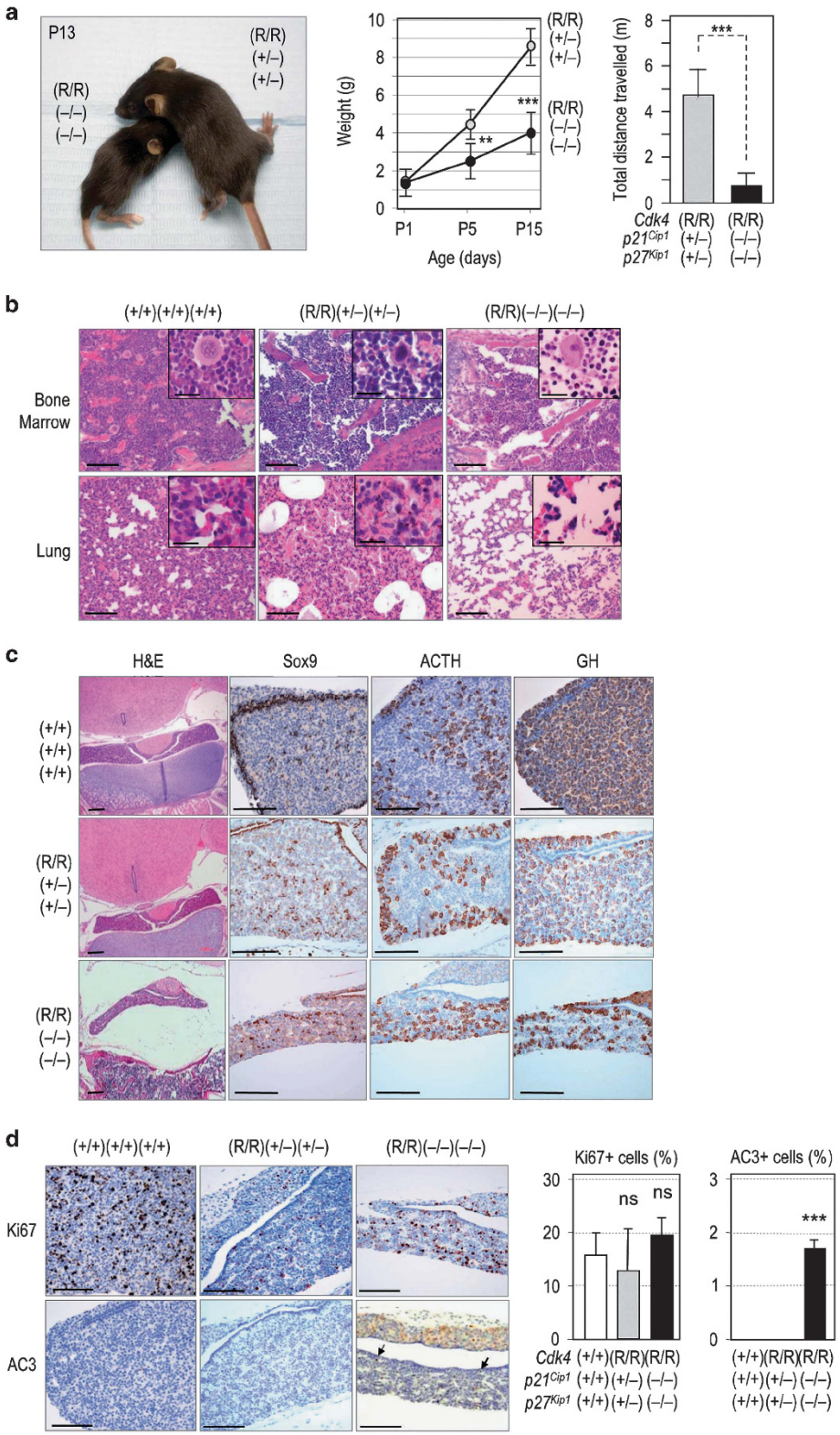

Figure 2 Perinatal pathologies in *Cdk4*(R/R); *p21*(–/–); *p27*(–/–) triple mutant mice. (**a**) Representative picture of a 13-day-old triple mutant mouse compared with a littermate. The weight of these animals at different ages is plotted (right panel; $n=6$ per genotype). The motility of P15 mice was assessed using the Open Field test ($n=6$ per genotype). (**b**) Representative micrographs showing bone marrow and lung hypoplasia mice with the indicated genotypes. Scale bars, 100 μm (insets, 20 μm). (**c**) Representative micrographs of the pituitary gland in newborn mice [postnatal day (P)5] of the indicated genotypes after staining with hematoxylin and eosin (H&E) or specific antibodies against Sox9 (a marker of pituitary progenitors;[45] adrenocorticotropic hormone (ACTH) or growth hormone (GH). (**d**) Quantification of proliferation (Ki67 staining) and apoptosis (active Caspase 3; AC3) in the sections of the pituitary gland of the indicated genotypes. Scale bars, 100 μm. In (**a**) and (**d**), Student's *t*-test, $^{**}P<0.01$; $^{***}P<0.001$

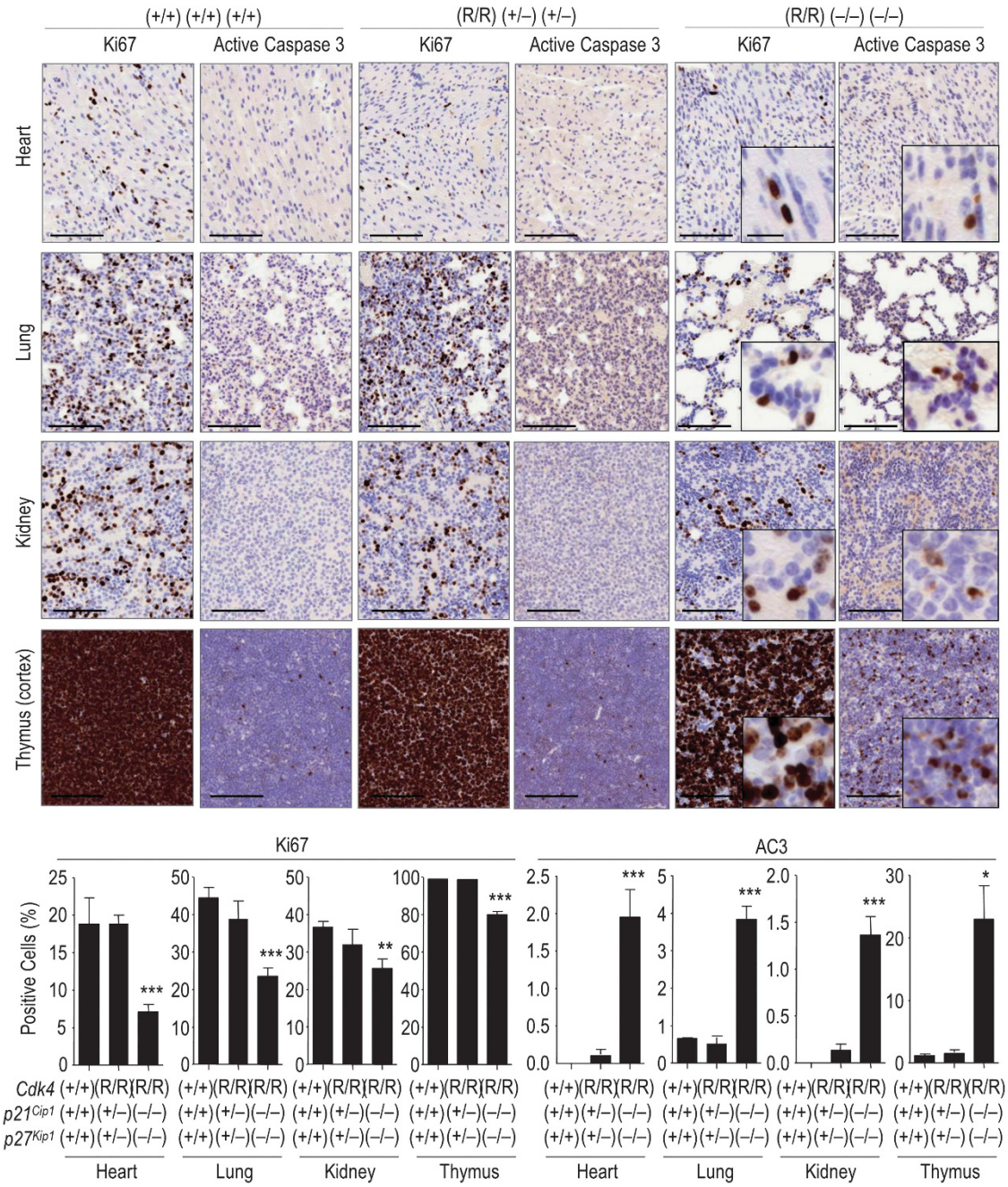

Figure 3 Wide-spread apoptosis in triple mutant tissues. Representative micrographs of several tissues in triple mutant mice showing defects in proliferation (Ki67 staining) and apoptosis (active caspase 3; AC3) by postnatal day 15 (P15). $^{*}P<0.05$; $^{**}P<0.01$; $^{***}P<0.001$; Student's *t*-test. Scale bars, 100 μm (insets 20 μm)

statistically significant, the consistent increase in EdU staining in *p21*(–/–) *and p21*(–/–);*p27*(–/–) neural progenitors correlates with the increased formation of primary neurospheres by these cells. Similarly, *Cdk4*(R/R) neural progenitors displayed reduced EdU levels in the presence of Cip/Kip inhibitors (Figure 6f) in correlation with the decreased potential in the formation of neurospheres (Figures 6a–e).

Surprisingly, EdU levels were significantly increased in triple mutant cells (Figure 6f) instead of the decrease expected attending to the self-renewal and size of the spheres. Since the number of Sox9-positive cells was increased in triple mutant neurospheres, it is possible that the increased EdU signal was due to the higher proliferative potential of these progenitors. However, triple mutant cells frequently displayed the pan-nuclear, intense γH2AX signal (Figure 6f), suggesting that the proliferative potential of Cdk4 R24C; p21-null; p27-null cells was hampered by the replicative stress caused by the lack of functional Ink4 and Cip/Kip inhibitors.

We next decided to use the immortalized mouse neural progenitor cell line C17.2 (ref. [26]) for more detailed molecular studies. Expression of Cdk4 R24C and concomitant knockdown of both $p21^{Cip1}$ and $p27^{Kip1}$ induced increased levels of

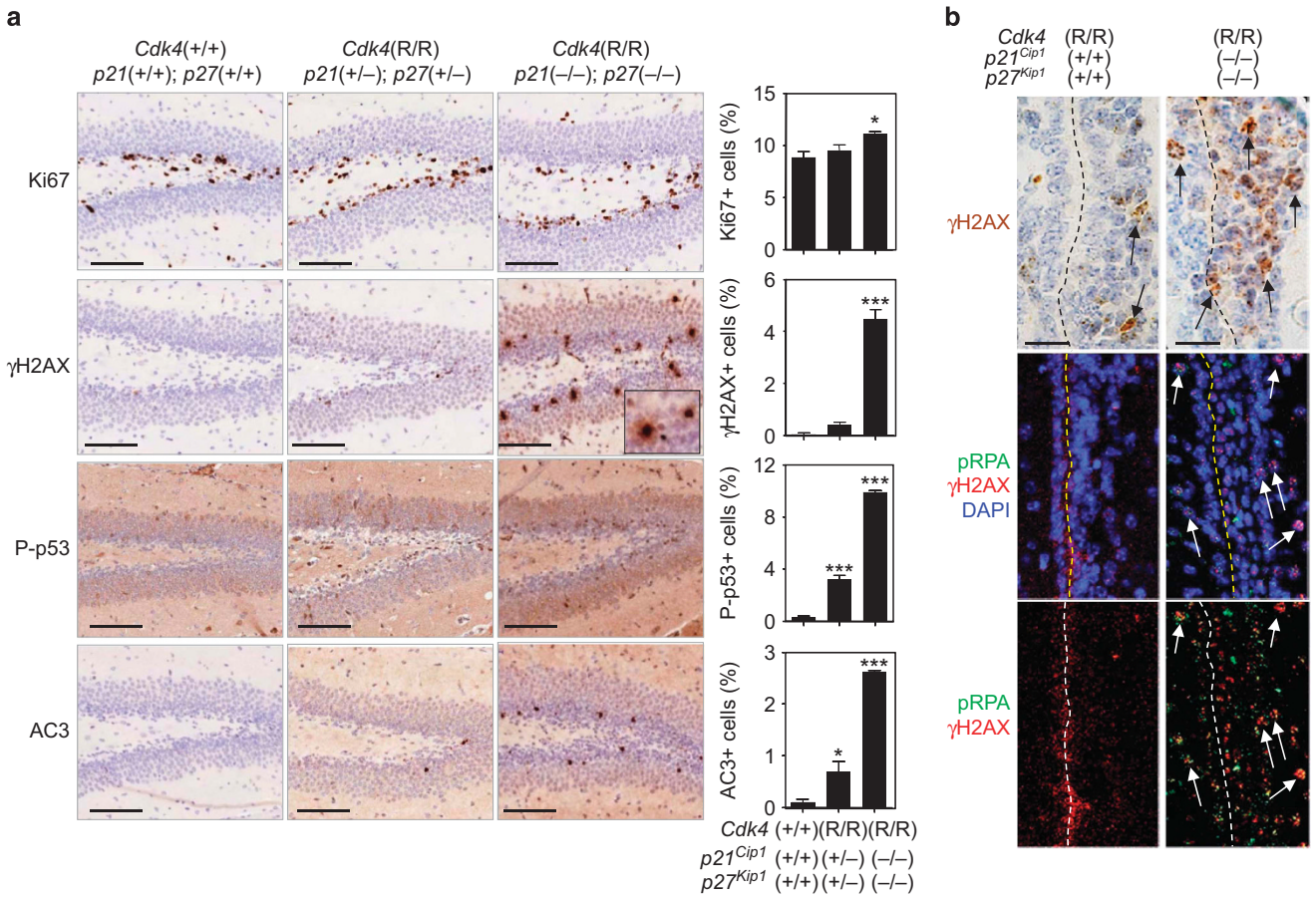

Figure 4 Increased replicative stress in neural progenitors at the hippocampus. (**a**) The dentate gyrus of the hippocampus was immunostained with antibodies against Ki67, phosphorylated H2AX (γH2AX), phosphorylated p53 (Ser15) and active Caspase 3 (AC3). The quantification of these signals (as percentage of positive cells) is shown in the corresponding histograms. Scale bar, 100 μm. $^{*}P<0.05$; $^{***}P<0.0001$. (**b**) Double staining for phosphorylated RPA (pRPA) and γH2AX (γH2AX) in the subpendymal zone of control and triple mutant mice. The presence of positive cells for the corresponding markers is indicated by arrows. Scale bar, 20 μm

γH2AX and 53BP1 foci (Figures 7a and b). These observations were not an indirect consequence of the induction of caspases since treatement with caspase inhibitors did not rescue the levels of 53BP1 foci (Supplementary Figure S5). Similarly, knock-down of $p21^{Cip1}$ and $p27^{Kip1}$ in Cdk4 R24C-expressing cells resulted in increased levels of phosphorylation of p53 in Ser 15 and active caspase 3 (Figure 7c).

The combined deficiency in Ink4 and Cip/Kip inhibitors in C17.2 cells resulted in increased phosphorylation of pRb in agreement with increased Cdk4/6 activity in these cells (Figure 7d). In control cells, inhibition of Cdk4/6 with the specific inhibitor PD-0332991 resulted in increased DNA damage response, likely as a consequence of abnormal entry into or progression through S-phase (Figure 7e). However, treatment with Cdk4/6 inhibitors in cells expressing Cdk4 R24C and knock-down for $p21^{Cip1}$ and $p27^{Kip1}$ led to reduced γH2AX signal, 53BP1 foci and decreased p53 activation (Figure 7e) in the presence of moderate phospho-pRb signal (Figure 7d). Altogether, these data suggest that the combination of the Cdk4 R24C allele with reduced levels of Cip/Kip inhibitors results in increased Cdk4/6 activity, replicative stress, and the induction of a p53 response and apoptotic cell death.

Discussion

One of the most frequent molecular events in human tumors is the deregulation of the cell cycle through Cdk hyperactivation. This may occur due to amplification, mutation or overexpression of cyclins and, more frequently, inactivation of Cdk inhibitors.[2] Members of the Ink4 family, mostly $p16^{Ink4a}$, $p15^{Ink4b}$ and $p18^{Ink4c}$, are frequently silenced in human cancer by deletion, mutation or epigenetic alterations. $p21^{Cip1}$ or $p27^{Kip1}$ inactivation may also occur through epigenetic alterations, increased proteolysis or as a consequence of defective p53 signaling.[2,6,27–29] The involvement of Ink4, Cip1 and Kip1 proteins in tumor development has been evaluated *in vivo* using different genetic mouse models. Genetic ablation of $p21^{Cip1}$ results in altered response to DNA damage responses and increased tumor susceptibility, specifically in mesenchymal and hematopoietic cells, at advanced age.[7,30] $p27^{Kip1}$ depletion in mice causes retinal dysplasia and female infertility and animals develop adenomas in the pituitary with long latencies.[8–10] The cooperation among these families has also been evaluated in different combinations. Mice deficient in $p18^{INK4c}$ in a $p21^{Cip1}$-*null* background cooperates in pituitary and lung tumors.[31] Combined ablation of $p18^{INK4c}$ and $p27^{Kip1}$ increases the frequency of endocrine and gut tumors.[15,31]

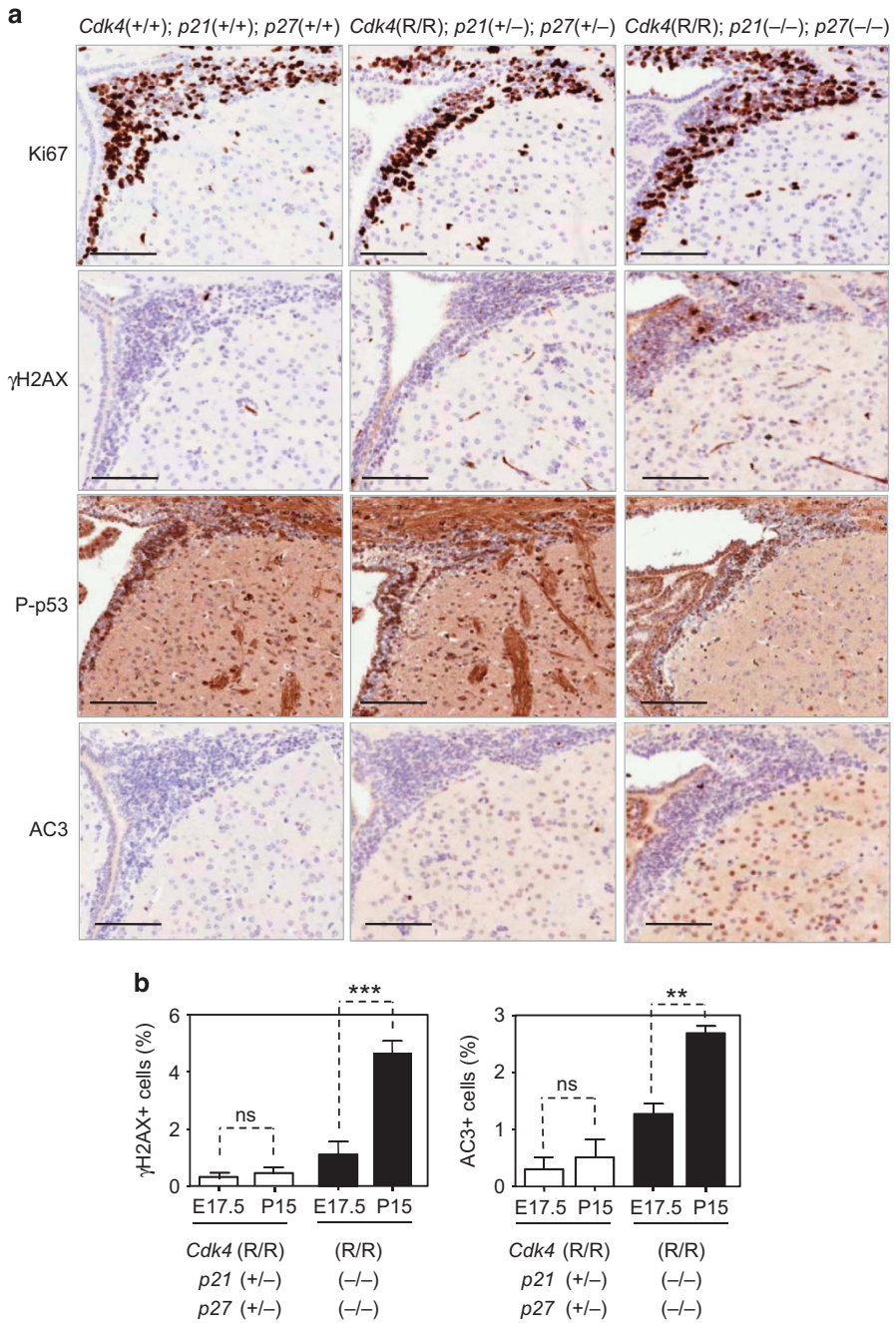

Figure 5 Increased replicative stress in neural progenitors at the subependymal zone of triple mutants. (**a**) The subependymal zone was immunostained with antibodies against Ki67, a proliferative marker, phosphorylated H2AX (γH2AX, which indicates DNA damage), phosphorylated p53 (Ser15; P-p53), and active Caspase 3 (AC3), a marker of apoptosis. Scale bar, 100 μm. (**b**) Comparison of the levels of γH2AX and AC3 in brains from E17.5 embryos and at postnatal day 15 (P15). ns, not significant; $^{**}P<0.01$; $^{***}P<0.001$; Student's *t*-test

On the other hand, the combined loss of $p21^{Cip1}$ and $p27^{Kip1}$ only has a modest effect in the latency of tumors.[23] Cdk4 R24C knock-in mice are a useful model since the endogenous Cdk4 protein is resistant to Ink4 family members in these animals.[19,32] Mice depleted for $p27^{Kip1}$ in a Cdk4 R24C background develop pituitary tumors with complete penetrance and very short latencies,[19,21] and ablation of $p21^{Cip1}$ in the Cdk4 R24C background accelerates mesenchymal tumor development.[22]

In this manuscript, we show that partial ablation of both $p21^{Cip1}$ and $p27^{Kip1}$ in a Cdk4 R24C background results in a synergistic effect in tumor development in a variety of tissues (Figure 1). Unexpectedly, complete ablation of $p21^{Cip1}$ and $p27^{Kip1}$ in the Cdk4 R24C background results in perinatal lethality in the absence of tumors, due to high levels of replicative stress accompanied by apoptotic cell death in multiple tissues. These results are in agreement with a model in which partial deregulation of cell-cycle inhibitors would

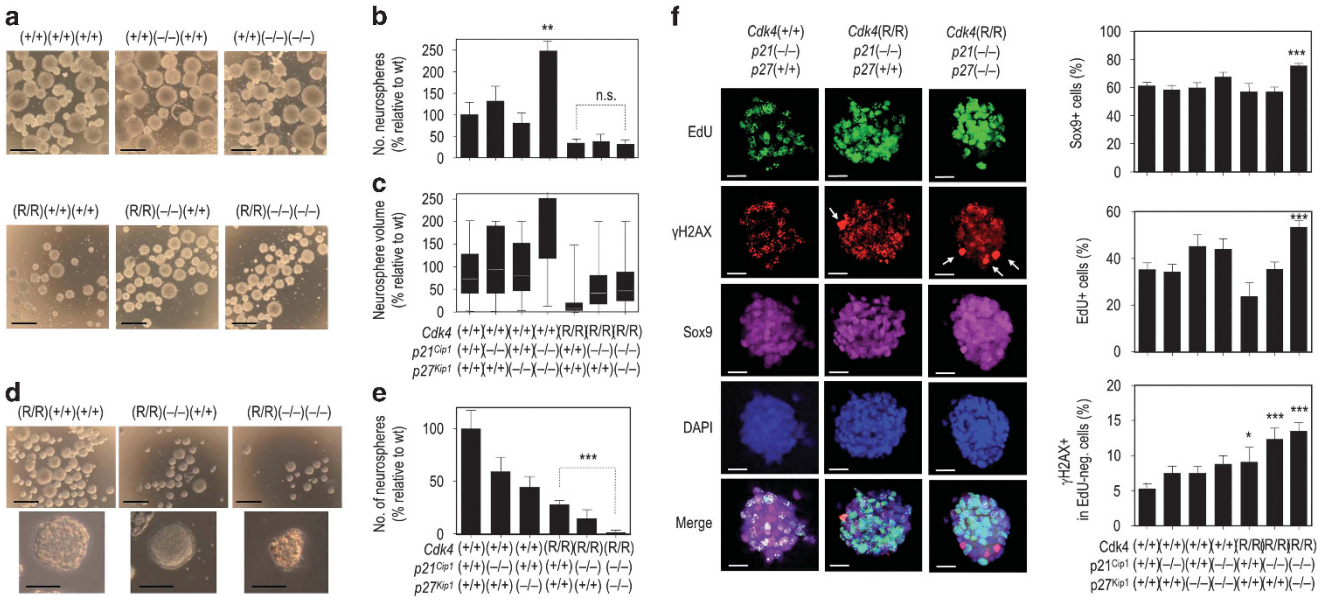

Figure 6 Self-renewal and proliferation defects in mutant neural progenitors. (**a**) Representative pictures of primary neurospheres of the indicated genotypes (following the Cdk4; p21; p27 order). Scale bars, 100 μm. The relative number of spheres formed from an equal number of neural progenitors (**b**) and the relative volume (**c**) of these neurospheres are represented in the histograms. The volume was calculated using the formula $4/3\pi r^3$ where r is the radius of the neurosphere calculated using Image J software. Neurospheres from at least three different clones were analyzed for each genotype. In (**b**) and (**c**), all genotypes display significant ($P<0.001$) differences when compared with wild types (wt), except the single p21 or p27 mutant neural progenitors. (**d**) Representative pictures of secondary cultures of indicated genotypes after disaggregation of the primary neurospheres. A representative secondary neurosphere is shown in the bottom panels. Scale bars, 100 μm (upper panels), 50 μm (bottom panels). (**e**) Quantification of the number of secondary neurospheres from the different genotypes. Lack of $p21^{Cip1}$ and $p27^{Kip1}$ in a *Cdk4*(R/R) background results in a significant defect in the number of secondary neurospheres when compared with *Cdk4*(R/R) mutants ($P<0.001$), whereas this effect was not significant in primary (**b**) cultures. (**f**) Replicative stress in *Cdk4*(R/R); *p21*(–/–); *p27*(–/–) triple mutant neural progenitors. Primary neurospheres were incubated in the presence of EdU for 1 h and seeded in a matrigel-coated coverslips for an additional 15 min. Immunofluorescence images (EdU, green; γH2AX, red; Sox 9, purple; and DAPI, blue) are shown for several representative genotypes. Cells with pan-staining for γH2AX indicating replicative stress are indicated by arrows. Scale bars, 20 μm. The quantification of cells positive for EdU, Sox 9 and γH2AX-positive cells within the EdU-negative population (to exclude cells in S-phase) is shown in the histograms. Error bars represents standard deviation from at least 10 spheres counted for each genotype (*$P<0.05$; **$P<0.01$; ***$P<0.001$)

result in acceleration of the cell cycle and would consequently lead to tumorigenesis. However, a minimum level of cell-cycle inhibitors is required for maintaining cell proliferation in these developing tissues. When cells reach that permissibility level, DNA synthesis is aberrant and cells eventually die probably as a consequence of the replicative stress generated. This is likely a consequence of enhanced Cdk4/6 activity as inhibition of these molecules decreases replicative stress and the subsequent p53-mediated response (Figure 7). Whereas we have not addressed the role of p53 in the generation of replicative stress in triple mutant mice, our previous results in Cdh1-deficient mice indicate that the replicative stress generated by enhanced Cdk activity is p53 independent, and suggest that p53 is only responsible for the apoptotic response to remove damaged cells from tissues.[33] p53 activation is known to result in either cell-cycle arrest, a pathway that involves the induction of $p21^{Cip1}$, or apoptotic cell death. As $p21^{Cip1}$ is absent in triple mutant mice, p53 signals are likely to favor apoptotic cell death instead of cell-cycle arrest in these mutant mice. However, the fact that *Cdk4*(R/R); *p21*(–/–); *p27*(+/+) mice do not display replicative stress or increased levels of apoptosis suggests that the major defect in triple mutant mice is not the alteration of the p53 pathway toward cell death, but the replicative stress generated in these mutant cells.

The relevance of cell-cycle inhibitors in preventing replicative stress may have important clinical implications in different tissues. Several brain diseases such as Alzheimer's disease or Seckel syndrome may be linked to replicative stress.[34,35] In the brain, Cip/Kip proteins have been involved in the regulation of neurogenesis and maintenance of neural stem cells homeostasis. $p27^{Kip1}$ is important for the proliferation and survival of postnatal neurons in the rostal migratory stream and to promote neurogenesis in the developing central nervous system.[36–38] $p21^{Cip1}$, on the other hand, can restrain neurogenesis in the subgranular zone of the dentate gyrus.[39] Hyperactivation of Cdk4 has been related to defects in neurogenesis and promotion of basal progenitor proliferation.[25] Homozygous deletion of the human locus encoding $p16^{Ink4a}$-$p19^{ARF}$-$p15^{Ink4b}$, often accompanied by deletion or mutation in $p18^{Ink4c}$, is among the most common genetic alterations in glioblastoma multiforme.[40] Inactivation of $p21^{Cip1}$ or $p27^{Kip1}$ is also common in different brain tumors[27,28,41] although a complete mapping of the concomitant silencing of Ink4 and Cip/Kip inhibitors in the same samples is not available at present.

Replicative stress is not only a defect that may be linked to developmental defects but it can also be used in therapy. Recently, it has been shown that oncogene-induced replicative stress can be used to selectively kill tumor cells.[42] Tumors with high levels of replicative stress, such as the ones generated by Myc overexpression, are specifically susceptible to genotoxic drugs that impair the DNA damage response

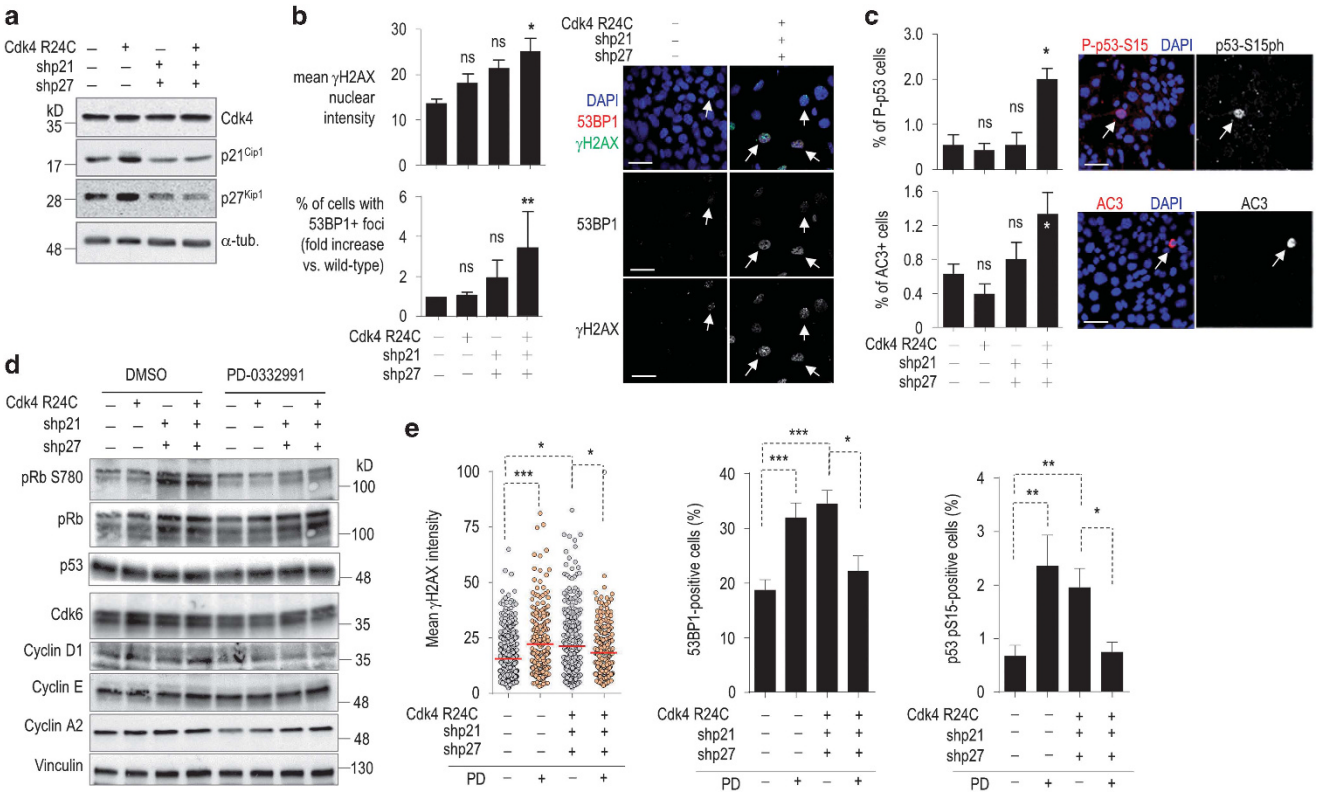

Figure 7 Combined effect of Cdk4 R24C expression and loss of Cip/Kip inhibitors in C17.2 cells. (**a**) C17.2 cells were transduced with virus expressing Cdk4 R24C or short-hairpin RNAs against p21^{Cip1} (shp21) and p27^{Kip1} (shp27). Downregulation of p21^{Cip1} and p27^{Kip1} was assessed by immunoblots. α-tubulin was used as a loading control. (**b**) Coexpression of Cdk4 R24C with short-hairpin RNAs against p21^{Cip1} (shp21) and p27^{Kip1} (shp27) results in increased phosphorylation of H2AX (γH2AX; $^*P<0.05$; one-way ANOVA) and increased percentage of cells with 53BP1 foci ($^*P<0.05$; Student's *t*-test). Data represent mean $\pm$ S.E.M. from three separate experiments. Representative images with double positive cells (arrows) are shown in the right panels. Scale bars, 20 μm. (**c**) Quantification of cells positive for p53 phosphorylation (S15ph) and active caspase 3 (AC3) in similar assays in C17.2 cells. Scale bars, 20 μm. $^*P<0.05$; Student's *t*-test. (**d**) Expression of Cdk4 R24C and downregulation of p21^{Cip1} and p27^{Kip1} result in increased phosphorylation of pRb (at Ser780). The protein level of additional cell-cycle regulators is also shown. pRb phosphorylation is reduced after treatment with the Cdk4/6 inhibitor PD-0332991 (1 μM). Vinculin was used as a loading control. (**e**) Effect of the inhibition of Cdk4/6 with PD-0332991 (1 μM PD) in the phosphorylation of H2AX (γH2AX), number of 53BP1 foci and p53 phosphorylation in control cells or cells expressing Cdk4 R24C and shRNAs against p21^{Cip1} and p27^{Kip1}. Data indicate mean $\pm$ S.D. from three independent experiments for PD and four for DMSO. One-way ANOVA $^*P<0.05$; $^{**}P<0.01$; $^{***}P<0.001$

pathway, such as Chk1 inhibitors currently in clinical trials. Similar strategies may be useful in brain tumors or other malignancies, in which multiple cell-cycle inhibitors are inactivated, to increase the levels of replicative stress with therapeutic purposes.

Materials and Methods

Mice and histological studies. Cdk4 R24C knock-in mice,[19] p21^{Cip1}-deficient[22,30] and p27^{Kip1}-deficient[10] animals have been reported previously. These animals were maintained in a mixed 129/Sv (25%) × CD1 (25%) × C57BL/6 J (50%) background. For the Open Field assay, the movement of P15 mice was recorded during 10 min in a square, white Plexiglas box. Mice were housed at the pathogen-free animal facility of the Centro Nacional de Investigaciones Oncológicas (Madrid) following the animal care standards of the institution. These animals were observed in a daily basis and sick mice were euthanized humanely in accordance with the Guidelines for Humane End Points for Animals used in biomedical research. Tumor latency has been considered equivalent to lifespan.

For histopathological observation, dissected organs were fixed in 10%-buffered formalin (Sigma, St. Louis, MO, USA) and embedded in paraffin wax. Three-micrometer-thick sections were stained with hematoxylin and eosin. Additional immunohistochemical examination of the pathologies observed was performed essentially as described in Sotillo *et al*.[21] Antibodies used for paraffin sections were glial-acidicic fibrilary protein, GFAP (1 : 500, Z0334; Dako, Glostrup, Denmark); Sox2 (1 : 400, AB5603; Millipore, Billerica, MA, USA); Ki67 (Prediluted, M7249; Dako); γH2AX (1 : 15 000, 05-636; Millipore); phospho-Ser15-p53 (1 : 25, Cell Signaling, Danvers, MA, USA); active Caspase 3 (1 : 400, AF835; R&D Systems, Minneapolis, MN, USA); beta-TSH (1 : 500, NIDDK, AFP-1274789); Growth hormone (1 : 50, NIDDK, AFP5672099Rb); ACTH (1 : 750, NIDDK, AFP156102789R) and PRL (1 : 150, NIDDK, AFP131078Rb).

Culture of neural progenitors. Neural progenitors were isolated from embryonic cortex as described previously.[43] Single dissociated cortical cells were cultured in uncoated 6-well plates between 1 and 2 weeks, in serum-free DMEM with 4.5 mg/ml glucose (Invitrogen, Waltham, MA, USA), 10 mM L-Glutamine (Invitrogen), 10 mM Na-Pyruvate (Invitrogen), 10 mM N-Acetyl Cysteine (Sigma), N2 supplement (Invitrogen), B27 supplement (Gibco, Waltham, MA, USA), EGF and bFGF (20 ng/ml each, Invitrogen). For subcloning, neurospheres were collected and gently dissociated using papain (Worthington, Lakewood, NJ, USA) at 37 °C for 20 min with gentle agitation. Cells were re-plated at equal cell density for each condition. The neural progenitor cell line C17.2 (ref. 26) was obtained from Sigma. C17.2 cells were transduced with retroviral vectors expressing Cdk4 R24C[22] or short-hairpin RNAs against p21^{Cip1} (ref. 44) or p27^{Kip1} (Sigma). Efficiency of the knock-down was tested by quantitative RT-PCR using SybrGreen.

Immunodetection of proteins. Neural progenitors were incubated with EdU (Invitrogen) at 10 μM for 1 h and then plated in a coverslip coated with matrigel (BD Bioscience, Franklin Lakes, NJ, USA). After 15 min in the matrigel, the spheres were attached to the coverslip. All incubations were performed at room temperature. Fixation of the spheres was done using PBS-4%PFA for 20 min. Spheres were permeabilized with PBS-TX100 0.5% for 15 min and blocked with PBS-3%

BSA-0.15%TX100 for 30 min. EdU staining was performed following provider guidelines (Invitrogen). For immunofluorescence, C17.2 cells were seeded on poly-L-lysine pre-coated glass coverslips and treated with 1 μM PD-0332991 HCl (SelleckChem, Houston, TX, USA) for 40 h or DMSO, after which cells were washed in PBS and fixed with 1% paraformaldehyde/1% sucrose for 20 min. Cells were permeabilized with 0.25% BSA, 0.5% Triton X-100 in PBS for 10 min and blocked with washing buffer 3% BSA for 1 h. Neurospheres or C17.2 cells were incubated with specific antibodies against Sox9 (1 : 250, Millipore, AB5535), phospho-RPA (1 : 100; S4/S8; Bethyl Laboratories, Montgomery, TX, USA), 53BP1 (1 : 100; ab36823; Abcam, Cambridge, UK), phospho-p53-Ser15 (1 : 100; Cell Signaling, 9284 S), $p21^{Cip1}$ (1 : 100, sc-6246, Santa Cruz Biotechnology, Santa Cruz, CA, USA), $p27^{Kip1}$ (1 : 100; BD Biosciences, 610241) and γH2AX (1 : 750, Millipore, 05-636), and secondary fluorescence antibodies (Alexa-594 goat anti-mouse and Alexa-647 goat anti-Rabbit; 1 : 250, Invitrogen). Cells were finally mounted in prolong anti-fade with DAPI (Invitrogen) and visualized using a confocal microscope SP2 (Leica, Wetzlar, Germany).

For immunoblots, C17.2 cells were treated with 1 μM PD-0332991 HCl (SelleckChem) for 40 h or DMSO, after which cells were washed in PBS and lysed in Laemmli's buffer. Protein concentration was determined with BCA protein assay (Pierce Biotechnology, Inc., Waltham, MA, USA). In all, 30 μg of total protein was loaded on 4–15% Mini-PROTEAN TGX Gels (BioRad, Hercules, CA, USA). The following primary antibodies were used for detection of proteins in these immunoblots: cyclin D1 (1 : 500; clone M-2, Santa Cruz Biotechnology, sc-718), Cyclin A2 (1:500; H-432, Santa Cruz Biotechnology, sc-751), Rb phospho-Ser 780 (1 : 250; Cell Signaling, 9307), Rb (1 : 250; G3-245, BD Biosciences, 554136), alpha-tubulin (1:2000; Sigma, T 9026), vinculin (1:2500; Sigma, V9131), Cdk4 (1 : 1000; Abcam, ab137675), cyclin E (1 : 1000; Abcam, ab7959-1), Cdk6 (a gift from M Barbacid), $p21^{Cip1}$ (1 : 250, sc-397, Santa Cruz Biotechnology), $p27^{Kip1}$ (1 : 1000; BD Biosciences, 610241), p53 (1 : 1000; Cell Signaling Technology, 2524). Horseradish peroxidase-conjugated goat anti-mouse and anti-rabbit immunoglobulins (Dako) were used as secondary antibodies.

Statistical analysis. Statistical significance was determined using Student' *t*-test unless otherwise indicated. $P<0.05$ (*), $P<0.01$ (**) and $P<0.001$ (***) were considered as significant (asterisks refer to all figures).

Conflict of Interest

The authors declare no conflict of interest.

Acknowledgements. We thank D Santamaría for critical comments on the manuscript. We thank Sally Temple and the members of her lab at the New York Neural Stem Cell Institute for guidelines in the work with neural progenitors. We also thank Beatriz Escobar and David Partida for excellent technical assistance, Sheila Rueda for colony mice management, and the members of the Confocal Microscopy and Comparative Pathology Units of the CNIO for their help. PD was supported by the Région Aquitaine and the Association pour la Recherche contre le Cancer (ARC). VQ was supported by fellowships from the Ministerio de Economía y Competitividad (MINECO). The Cell Division and Cancer group of the CNIO is funded by the MINECO (SAF2012-38215), Red Temática CellSYS (BFU2014-52125-REDT) and Red Consolider OncoBIO (SAF2014-57791-REDC), Comunidad de Madrid (OncoCycle Programme, S2010/BMD-2470), Worldwide Cancer Research (WCR #15-0278) and the EU MitoSys project (HEALTH-F5-2010-241548; European Union Seventh Framework Program).

1. Sherr CJ. The Pezcoller lecture: cancer cell cycles revisited. *Cancer Res* 2000; **60**: 3689–3695.
2. Malumbres M, Barbacid M. To cycle or not to cycle: a critical decision in cancer. *Nat Rev Cancer* 2001; **1**: 222–231.
3. Malumbres M, Barbacid M. Cell cycle, CDKs and cancer: a changing paradigm. *Nat Rev Cancer* 2009; **9**: 153–166.
4. Malumbres M, Barbacid M. Mammalian cyclin-dependent kinases. *Trends Biochem Sci* 2005; **30**: 630–641.
5. Sherr CJ, Roberts JM. CDK inhibitors: positive and negative regulators of G1-phase progression. *Genes Dev* 1999; **13**: 1501–1512.
6. Ruas M, Peters G. The p16INK4a/CDKN2A tumor suppressor and its relatives. *Biochim Biophys Acta* 1998; **1378**: F115–F177.
7. Martin-Caballero J, Flores JM, Garcia-Palencia P, Serrano M. Tumor susceptibility of p21 (Waf1/Cip1)-deficient mice. *Cancer Res* 2001; **61**: 6234–6238.
8. Nakayama K, Ishida N, Shirane M, Inomata A, Inoue T, Shishido N *et al.* Mice lacking p27 (Kip1) display increased body size, multiple organ hyperplasia, retinal dysplasia, and pituitary tumors. *Cell* 1996; **85**: 707–720.
9. Fero ML, Rivkin M, Tasch M, Porter P, Carow CE, Firpo E *et al.* A syndrome of multiorgan hyperplasia with features of gigantism, tumorigenesis, and female sterility in p27(Kip1)-deficient mice. *Cell* 1996; **85**: 733–744.
10. Kiyokawa H, Kineman RD, Manova-Todorova KO, Soares VC, Hoffman ES, Ono M *et al.* Enhanced growth of mice lacking the cyclin-dependent kinase inhibitor function of p27(Kip1). *Cell* 1996; **85**: 721–732.
11. Latres E, Malumbres M, Sotillo R, Martín J, Ortega S, Martín-Caballero J *et al.* Limited overlapping roles of P15(INK4b) and P18(INK4c) cell cycle inhibitors in proliferation and tumorigenesis. *EMBO J* 2000; **19**: 3496–3506.
12. Sharpless NE, Bardeesy N, Lee KH, Carrasco D, Castrillon DH, Aguirre AJ *et al.* Loss of p16Ink4a with retention of p19Arf predisposes mice to tumorigenesis. *Nature* 2001; **413**: 86–91.
13. Krimpenfort P, Quon KC, Mooi WJ, Loonstra A, Berns A. Loss of p16Ink4a confers susceptibility to metastatic melanoma in mice. *Nature* 2001; **413**: 83–86.
14. Krimpenfort P, Ijpenberg A, Song JY, van der Valk M, Nawijn M, Zevenhoven J *et al.* p15Ink4b is a critical tumour suppressor in the absence of p16Ink4a. *Nature* 2007; **448**: 943–946.
15. Franklin DS, Godfrey VL, Lee H, Kovalev GI, Schoonhoven R, Chen-Kiang S *et al.* CDK inhibitors p18(INK4c) and p27(Kip1) mediate two separate pathways to collaboratively suppress pituitary tumorigenesis. *Genes Dev* 1998; **12**: 2899–2911.
16. Ramsey MR, Krishnamurthy J, Pei XH, Torrice C, Lin W, Carrasco DR *et al.* Expression of p16Ink4a compensates for p18Ink4c loss in cyclin-dependent kinase 4/6-dependent tumors and tissues. *Cancer Res* 2007; **67**: 4732–4741.
17. Martin-Caballero J, Flores JM, Garcia-Palencia P, Collado M, Serrano M. Different cooperating effect of p21 or p27 deficiency in combination with INK4a/ARF deletion in mice. *Oncogene* 2004; **23**: 8231–8237.
18. Wolfel T, Hauer M, Schneider J, Serrano M, Wölfel C, Klehmann-Hieb E *et al.* A p16INK4a-insensitive CDK4 mutant targeted by cytolytic T lymphocytes in a human melanoma. *Science* 1995; **269**: 1281–1284.
19. Sotillo R, Dubus P, Martin J, de la Cueva E, Ortega S, Malumbres M *et al.* Wide spectrum of tumors in knock-in mice carrying a Cdk4 protein insensitive to INK4 inhibitors. *EMBO J* 2001; **20**: 6637–6647.
20. Sotillo R, Garcia JF, Ortega S, Martin J, Dubus P, Barbacid M *et al.* Invasive melanoma in Cdk4-targeted mice. *Proc Natl Acad Sci USA* 2001; **98**: 13312–13317.
21. Sotillo R, Renner O, Dubus P, Ruiz-Cabello J, Martín-Caballero J, Barbacid M *et al.* Cooperation between Cdk4 and p27kip1 in tumor development: a preclinical model to evaluate cell cycle inhibitors with therapeutic activity. *Cancer Res* 2005; **65**: 3846–3852.
22. Quereda V, Martinalbo J, Dubus P, Carnero A, Malumbres M. Genetic cooperation between p21Cip1 and INK4 inhibitors in cellular senescence and tumor suppression. *Oncogene* 2007; **26**: 7665–7674.
23. Garcia-Fernandez RA, Garcia-Palencia P, Sanchez MA, Gil-Gómez G, Sánchez B, Rollán E *et al.* Combined loss of p21(waf1/cip1) and p27(kip1) enhances tumorigenesis in mice. *Lab Invest* 2011; **91**: 1634–1642.
24. Quereda V, Malumbres M. Cell cycle control of pituitary development and disease. *J Mol Endocrinol* 2009; **42**: 75–86.
25. Lange C, Huttner WB, Calegari F. Cdk4/cyclinD1 overexpression in neural stem cells shortens G1, delays neurogenesis, and promotes the generation and expansion of basal progenitors. *Cell Stem Cell* 2009; **5**: 320–331.
26. Ryder EF, Snyder EY, Cepko CL. Establishment and characterization of multipotent neural cell lines using retrovirus vector-mediated oncogene transfer. *J Neurobiol* 1990; **21**: 356–375.
27. Chu IM, Hengst L, Slingerland JM. The Cdk inhibitor p27 in human cancer: prognostic potential and relevance to anticancer therapy. *Nat Rev Cancer* 2008; **8**: 253–267.
28. Coqueret O. New roles for p21 and p27 cell-cycle inhibitors: a function for each cell compartment? *Trends Cell Biol* 2003; **13**: 65–70.
29. Gil J, Peters G. Regulation of the INK4b-ARF-INK4a tumour suppressor locus: all for one or one for all. *Nat Rev Mol Cell Biol* 2006; **7**: 667–677.
30. Brugarolas J, Chandrasekaran C, Gordon JI, Beach D, Jacks T, Hannon GJ. Radiation-induced cell cycle arrest compromised by p21 deficiency. *Nature* 1995; **377**: 552–557.
31. Franklin DS, Godfrey VL, O'Brien DA, Deng C, Xiong Y. Functional collaboration between different cyclin-dependent kinase inhibitors suppresses tumor growth with distinct tissue specificity. *Mol Cell Biol* 2000; **20**: 6147–6158.
32. Rodriguez-Diez E, Quereda V, Bellutti F, Prchal-Murphy M, Partida D, Eguren M *et al.* Cdk4 and Cdk6 cooperate in counteracting the INK4 family of inhibitors during murine leukemogenesis. *Blood* 2014; **124**: 2380–2390.
33. Eguren M, Porlan E, Manchado E, García-Higuera I, Cañamero M, Fariñas I *et al.* The APC/C cofactor Cdh1 prevents replicative stress and p53-dependent cell death in neural progenitors. *Nat Commun* 2013; **4**: 2880.
34. Yurov YB, Vorsanova SG, Iourov IY. The DNA replication stress hypothesis of Alzheimer's disease. *ScientificWorldJournal* 2011; **11**: 2602–2612.
35. Murga M, Bunting S, Montana MF, Soria R, Mulero F, Cañamero M *et al.* A mouse model of ATR-Seckel shows embryonic replicative stress and accelerated aging. *Nat Genet* 2009; **41**: 891–898.

36. Farah MH, Olson JM, Sucic HB, Hume RI, Tapscott SJ, Turner DL. Generation of neurons by transient expression of neural bHLH proteins in mammalian cells. *Development* 2000; **127**: 693–702.
37. Li X, Tang X, Jablonska B, Aguirre A, Gallo V, Luskin MB. p27(KIP1) regulates neurogenesis in the rostral migratory stream and olfactory bulb of the postnatal mouse. *J Neurosci* 2009; **29**: 2902–2914.
38. Zheng YL, Li BS, Rudrabhatla P, Shukla V, Amin ND, Maric D *et al.* Phosphorylation of p27Kip1 at Thr187 by cyclin-dependent kinase 5 modulates neural stem cell differentiation. *Mol Biol Cell* 2010; **21**: 3601–3614.
39. Pechnick RN, Zonis S, Wawrowsky K, Pourmorady J, Chesnokova V. p21Cip1 restricts neuronal proliferation in the subgranular zone of the dentate gyrus of the hippocampus. *Proc Natl Acad Sci USA* 2008; **105**: 1358–1363.
40. Solomon DA, Kim JS, Jean W, Waldman T. Conspirators in a capital crime: co-deletion of p18INK4c and p16INK4a/p14ARF/p15INK4b in glioblastoma multiforme. *Cancer Res* 2008; **68**: 8657–8660.
41. Bhatia B, Malik A, Fernandez LA, Kenney AM. p27(Kip1), a double-edged sword in Shh-mediated medulloblastoma: Tumor accelerator and suppressor. *Cell Cycle* 2010; **9**: 4307–4314.
42. Murga M, Campaner S, Lopez-Contreras AJ, Toledo LI, Soria R, Montaña MF *et al.* Exploiting oncogene-induced replicative stress for the selective killing of Myc-driven tumors. *Nat Struct Mol Biol* 2011; **18**: 1331–1335.
43. Qian X, Shen Q, Goderie SK, He W, Capela A, Davis AA *et al.* Timing of CNS cell generation: a programmed sequence of neuron and glial cell production from isolated murine cortical stem cells. *Neuron* 2000; **28**: 69–80.
44. Trakala M, Fernandez-Miranda G, Perez de Castro I, Heeschen C, Malumbres M. Aurora B prevents delayed DNA replication and premature mitotic exit by repressing p21(Cip1). *Cell Cycle* 2013; **12**: 1030–1041.
45. Garcia-Lavandeira M, Quereda V, Flores I, Saez C, Diaz-Rodriguez E, Japon MA *et al.* A GRFa2/Prop1/stem (GPS) cell niche in the pituitary. *PLoS One* 2009; **4**: e4815.

Supplementary Information accompanies this paper on Cell Death and Differentiation website (http://www.nature.com/cdd)